Cardiovasc Intervent Radiol (2019) 42:591–600
https://doi.org/10.1007/s00270-018-2116-8

CLINICAL INVESTIGATION IMAGING

Comparative Analysis of Intra-arterial Cone-Beam Versus Conventional Computed Tomography During Hepatic Arteriography for Transarterial Chemoembolization Planning

Ethan Y. Lin[1] · A. Kyle Jones[2] · Gouthami Chintalapani[3] · Zachary S. Jeng[4] · Joe Ensor[5] · Bruno C. Odisio[1]

Received: 11 September 2018 / Accepted: 2 November 2018 / Published online: 9 November 2018

Abstract

Purpose To compare the imaging characteristics of intra-arterial cone-beam computed tomography during hepatic arteriography (CBCTHA) versus intra-arterial computed tomography during hepatic arteriography (CTHA) for intraprocedural transarterial chemoembolization (TACE) planning.

Materials and Methods This single-institution retrospective study included 144 patients (96 men, mean age 67.9 years; 48 women, mean age 62.3 years) who underwent 181 TACE sessions between January 2015 and July 2017. Intraprocedural CBCTHA (111 procedures) or CTHA (70 procedures) was performed for TACE planning. Reformatted maximum intensity projection CBCTHA and CTHA images were reviewed by two radiologists and classified using an ordinal scoring system (for tumor identification, tumor feeder vessel identification, and streaking artifact) and a binary scoring system (for the presence of breathing motion artifact and field of view encompassing the entire liver). Data were analyzed using an F test and a z-score test.

Results There were no significant differences in demographic and tumor characteristics between the CBCTHA and CTHA patient cohorts. CTHA was superior to CBCTHA for tumor identification ($P < .0001$), tumor feeder vessel identification ($P < .05$), streaking artifact ($P < .0001$), and field of view encompassing the entire liver ($P < .0001$). There was a trend toward a lower frequency of breathing motion artifact with CTHA than with CBCTHA (1.4% vs. 10%; $P = .057$).

Conclusion CTHA provides improved clinical relevant imaging information compared to CBCTHA for intraprocedural TACE planning.

Level of Evidence Level III, retrospective comparative study.

Keywords Cone-beam computed tomography · Helical computed tomography · Computed tomography angiography · Therapeutic chemoembolization · Neoplasms

✉ Bruno C. Odisio
BCOdisio@mdanderson.org

[1] Department of Interventional Radiology, The University of Texas MD Anderson Cancer Center, 1515 Holcombe Blvd, Houston, TX 77030, USA

[2] Department of Imaging Physics, The University of Texas MD Anderson Cancer Center, 1515 Holcombe Blvd, Houston, TX 77030, USA

[3] Siemens Medical Solutions USA Inc., 2501 North Barrington Road, Hoffman Estates, IL 60192, USA

[4] Department of Radiology, Baylor College of Medicine, 1 Baylor Plaza, Houston, TX 77030, USA

[5] The Houston Methodist Research Institute, 6670 Bertner Ave, Houston, TX 77030, USA

Introduction

Cross-sectional imaging (CSI) during transarterial hepatic procedures has become a critical tool in interventional oncology given its ability to offer relevant information for tumor identification, assessment of tumor blood supply, navigation guidance, and intraprocedural tumor response assessment [1, 2]. Since its inception, considerable

improvements in image quality and workflow have occurred [3, 4]. Specifically, the development of hybrid angiography-computed tomography (hybrid angio-CT) systems [5] and flat-panel X-ray detector angiographic systems with cone-beam CT (CBCT) imaging capabilities [6, 7] has substantially improved procedural workflow by obviating the need for patient transportation to a dedicated CT room, while providing high-quality intraprocedural soft tissue cross-sectional imaging [8].

Fundamental differences exist between CBCT and CT in respect of imaging characteristics. Compared to CT, CBCT is associated with a smaller field of view (FOV) and reduced z-axis scanning, which limits the volume of the liver that can be imaged; also, the longer rotation time and reduced angular sampling on CBCT might also increase the frequency and severity of motion artifacts [9, 10]. The use of CBCT and hybrid angio-CT has also historically differed by geographical location, with most hybrid angio-CT systems been used in Asia [1, 11–14], while CBCT being the standard cross-sectional imaging modality in the Western world [2].

The use of cone-beam CT during hepatic arteriography (CBCTHA) during transarterial hepatic procedures has been part of our institution's practice since 2008. With the recent incorporation of two hybrid angio-CT systems in 2016, computed tomography during hepatic arteriography (CTHA) was added as an alternative to CBCTHA for cross-sectional imaging during transarterial hepatic procedures. Although radiation dose and imaging quality of CBCT and CT were compared in phantom study [15], there have been no clinical studies comparing cross-sectional imaging characteristics between CBCT and hybrid angio-CT during transarterial hepatic procedures. It is currently unknown which imaging modality provides pivotal information during transarterial chemoembolization procedures. Therefore, the purpose of this study was to perform a qualitative comparative imaging quality analysis of intra-arterial CBCTHA versus CTHA for transarterial (chemo)embolization (TACE) planning.

Materials and Methods

Study Population

This single-institution retrospective study was compliant with the Health Insurance Portability and Accountability Act and approved by our Institutional Review Board with a waiver of informed consent. Our institution's TACE database was retrospectively searched to identify consecutive TACE procedures performed from January 2015 through July 2017. Based on our Institutional protocol, patients with hypervascular lesions on pre-TACE were selected to receive TACE. As per our standard of care protocol,

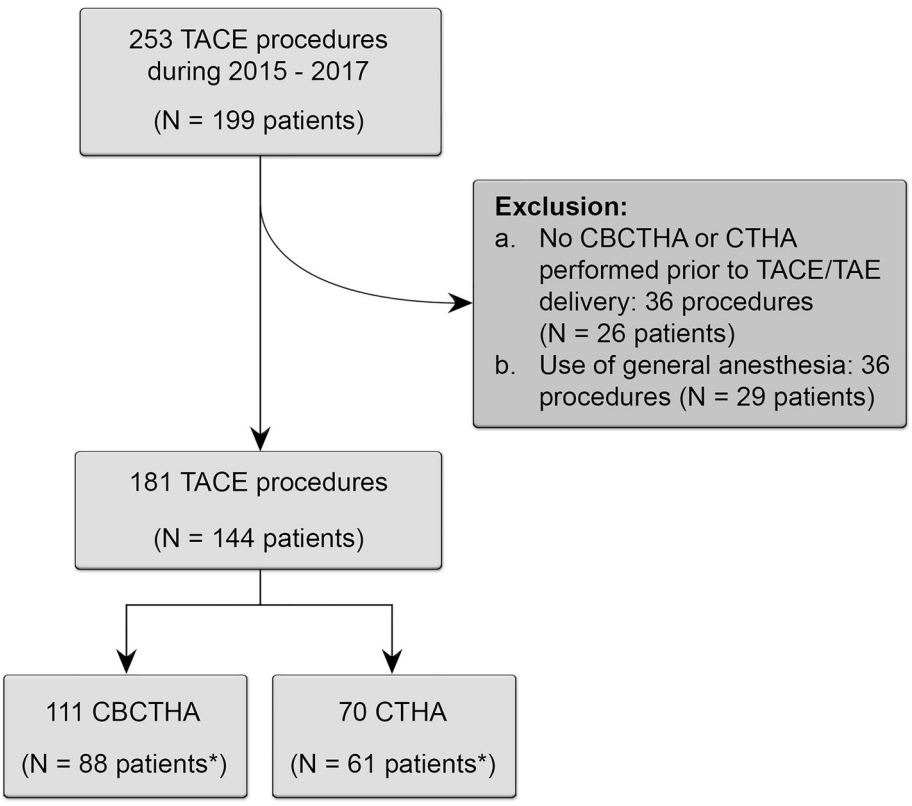

Fig. 1 Flowchart of patient selection. *Five patients underwent both CBCTHA and CTHA

Table 1 Patient demographics and clinical characteristics ($N = 144$)

Parameter	CBCTHA	CTHA	*P* value
No. of patients[a]	88	61	
Sex, no. (%)			.59
Male	57 (65)	42 (69)	
Female	31 (35)	19 (31)	
Age, mean ± SD	65.5 ± 11.1	66.6 ± 10.0	.50
BMI, mean ± SD	28.0 ± 7.0	27.3 ± 5.0	.56
Largest tumor size[b], mean ± SD (cm)	4.9 ± 2.9	4.7 ± 3.3	.73
Total number of tumors per patient, mean ± SD	2.3 ± 2.4	3.3 ± 3.7	.06
Type of malignancy, no. (%)			.14
HCC	51 (58)	43 (71)	
mCRC	4 (5)	0 (0)	
Neuroendocrine tumor	2 (2)	3 (5)	
Melanoma	13 (15)	6 (10)	
Intrahepatic CCA	5 (6)	1 (2)	
Other	13 (15)	8 (13)	
No. of TACE procedures	111	70	
Prior TACE, no. (%)			.93
No	61 (55)	38 (54)	
Yes	50 (45)	32 (46)	
CSI before TACE, no. (%)			.15
CT	88 (80)	48 (69)	
MRI	23 (21)	22 (31)	
Catheter tip location			.01
Proximal to GDA	40 (36)	38 (54)	
Celiac trunk	16 (14)	19 (27)	
Common HA	24 (22)	19 (27)	
Distal to GDA	71 (64)	32 (46)	
Proper HA	21 (19)	13 (19)	
Lobar HA	45 (41)	17 (24)	
Segmental HA	5 (5)	2 (3)	

[a]Five patients had both CBCT and hybrid angio-CT. The score test was generated from the generalized estimating equations produced by fitting a generalized linear model with a subject effect to account for the five-patient overlap between the two treatment cohorts

[b]Measurements taken on CBCTHA and CTHA imaging

BMI body mass index, *CBCTHA* cone-beam computed tomography during hepatic arteriography, *CCA* cholangiocarcinoma, *CSI* cross-sectional imaging, *CT* computed tomography, *CTHA* computed tomography during hepatic arteriography, *GDA* gastroduodenal artery, *HA* hepatic artery, *mCRC* colorectal cancer liver metastasis, *MRI* magnetic resonance imaging, *SD* standard deviation, *TACE* transarterial chemoembolization

patients eligible for TACE had either a quadriphasic contrast-enhanced CT or a dynamic magnetic resonance image (MRI) performed within 8 weeks from the TACE procedure.

A total of 253 consecutive TACE procedures in 199 patients were identified. After exclusion of procedures without CBCTHA or CTHA imaging planning and procedures in which general anesthesia was used, 181 TACE procedures (111 with CBCTHA planning and 70 with CTHA planning) in 144 patients were included in this study. Most patients received either CBCTHA or CTHA except five patients had both CBCTHA and CTHA (Fig. 1). The demographic and clinical characteristics of the 144 patients in the study are summarized in Table 1. The use of CBCTHA or CTHA depended on room availability and operator's preference. Patient's characteristics were not taken into consideration to decide using CBCTHA or CTHA. Patients who had CBCTHA and those who had CTHA did not differ significantly with respect to any of the characteristics measured except catheter tip

Table 2 Grading scale for tumor identification, tumor feeder vessel identification, and presence and effect of streaking artifact

Variable and grade	Definition
Tumor identification	
1	Target tumor(s) not identified per contrast enhancement on intraprocedural CBCTHA or CTHA compared to pre-procedure CSI
2	Target tumor(s) partially identified in extension OR number on intraprocedural CBCTHA or CTHA compared to pre-procedure CSI
3	Target tumor(s) fully detected in extension AND number on intraprocedural CBCTHA or CTHA compared to pre-procedure CSI
Tumor feeder vessel identification[a]	
1	No artery detected within 1 cm of periphery of target tumor(s)
2	Artery within 1 cm of periphery of target tumor(s) without direct contact with tumor(s)
3	Direct contact of artery with target tumor(s)
Streaking artifact	
1	Presence of streaking artifact with image quality degradation at target tumor(s)
2	Presence of streaking artifact without image quality degradation at target tumor(s)
3	No streaking artifact

[a]If no tumor was identified on CBCTHA or CTHA, the expected location of the tumor was used to determine the relationship between the artery and the tumor

CBCTHA cone-beam computed tomography during hepatic arteriography, *CSI* cross-sectional imaging, *CTHA* computed tomography during hepatic arteriography

location for intra-arterial injection. Because of the smaller FOV on CBCTHA, the higher frequency of catheter positioning distal to the gastroduodenal artery was found in the CBCTHA cohort.

Imaging Acquisition Protocol

Following intra-arterial access and catheterization, digital subtraction angiography was performed to identify hepatic arterial feeders and determine optimal injection parameters for delineating the feeding artery or arteries and opacifying the target tumor or tumors. Both CBCTHA and CTHA were acquired on expiration with breath hold during a single-phase acquisition using undiluted contrast medium (Omnipaque 300, GE Healthcare) injected at 2–3 mL/s for a total volume of 24–42 mL with an acquisition delay of 6 s in CBCTHA cohort and 8 s in CTHA cohort. The contrast medium injection rate was determined by subjective judgment of individual operator based on digital subtraction angiography performed with the same catheter at the same location where CBCTHA or CTHA was expected to be acquired. The total contrast medium injection time was 12–14 s. Contrast medium was injected with a power injector using either a 5F catheter (celiac trunk or common hepatic artery) or a 2.4F (right or left hepatic arteries) to 2.8F (common or proper hepatic arteries) co-axial microcatheter.

CBCTHA was performed with the patient's arms positioned above the head on a single-plane angiography system equipped with a 30 × 40 cm flat detector (Artis Zeego system or Artis Q ceiling-mounted system, Siemens Healthineers) using the default CBCT organ program parameters: 6-s or 8-s rotation time; 200° rotation; .5° angular step size; 397 (6 s) projections; detector dose level of .36 μGy/frame; and 660 × 480 acquisition matrix. The images were reconstructed on a dedicated workstation (XWP, Siemens Healthineers) using the default reconstruction preset, resulting in a stack of 512 × 512 matrices with an isotropic voxel size of .49 mm^3.

CTHA was performed with the patient's arms alongside the body on a 128-slice multidetector sliding-gantry CT scanner (SOMATOM Definition Edge SG, Siemens Healthineers) as part of a hybrid angio-CT suite (MIYABI angio-CT, Siemens Healthineers) with the following acquisition parameters: 120 kV; tube current modulation enabled with quality reference of 300 mAs; .5-s gantry rotation time; pitch .6; detector configuration of 128 × .6 mm; and scan time 4–6 s for the entire liver. The images were reconstructed using an iterative reconstruction algorithm (SAFIRE, Siemens Healthineers) with strength 3 and B40f medium convolution kernel.

Image Qualitative Assessment

CBCTHA and CTHA datasets were reviewed as 5-mm-thick maximum intensity projection images at soft tissue window settings on a dedicated workstation (XWP, Siemens Healthineers). A classification system was created by two interventional radiologists and one physicist with 7, 10, and 12 years of experience, respectively, using a modified classification system previously described for fluoroscopic and digital subtraction angiography image quality assessment [16]. This assessment included a three-grade ordinal scoring system (Table 2) for three distinct variables deemed relevant for TACE planning: *tumor identification* (Fig. 2), *tumor feeder vessel identification* (Fig. 3), and *presence and effect of streaking artifact* (Fig. 4). On patients with multiple tumors, the worst grading criteria for tumor identification was selected as the categorical variable. If no tumor was identified on CBCTHA or CTHA (grade 1 tumor identification), the expected location of the tumor was used to determine the tumor feeder vessel identification.

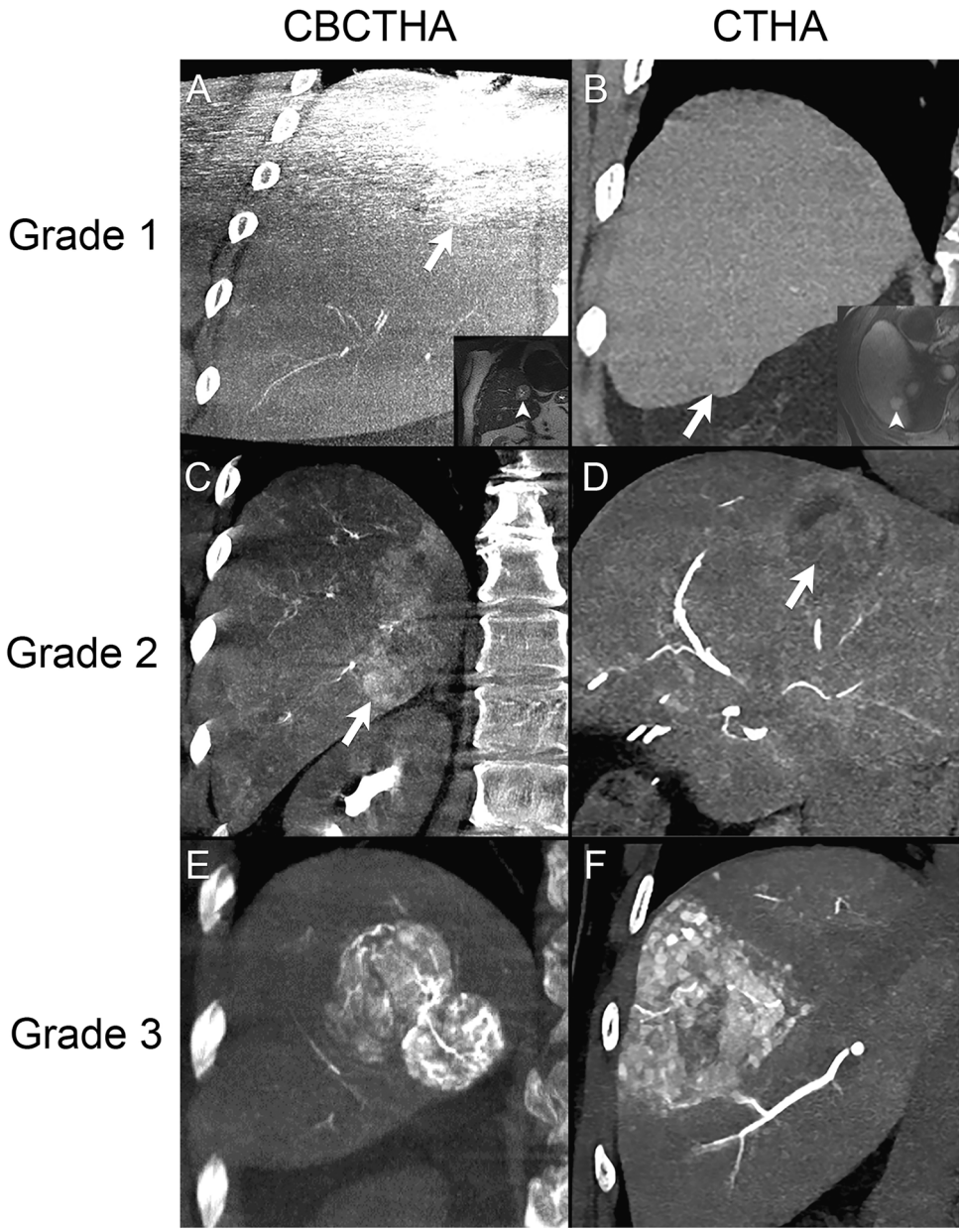

Fig. 2 Representative examples of grades 1, 2, and 3 tumor identification at a window width of 400 HU and level of 150 HU on coronal CBCTHA and coronal CTHA. **A** A neuroendocrine liver metastasis (inset, MR T2 sequence coronal showing the lesion [arrowhead]) at segment VIII of the liver was not identified visualized on CBCTHA (arrow); **B** A HCC at segment VI of the liver was poorly visualized on CTHA (arrow) but visualized as an early enhancing tumor on pre-TACE arterial-phase axial MRI (inset, arrowhead). **C** A HCC (arrow) was not fully opacified on CBCTHA. The left boundary of the tumor was not clear. **D** The superior margin of the HCC (arrow) was not well defined owing to partial enhancement of the tumor on CTHA. **E** Two HCCs were well enhanced with clear borders on CBCTHA. **F** A large HCC and multiple satellite nodules were well enhanced with clear borders on CTHA

Grading tumor identification was based on the visualization of tumor in extension and/or number. Grading tumor feeder vessel identification depended on direct contact of artery with target tumor(s), suspicious arterial feeders detected within 1 cm of the periphery of target tumor(s) or not. Streaking artifact was classified by the presence of streaking artifact with or without key image quality degradation at target tumor(s) or no streaking artifact.

The modified classification system also included a categorical binary scoring system (yes vs. no) for the *presence of breathing motion artifact* (Fig. 5) and *FOV encompassing the entire liver*. Subsequently, the two interventional radiologists independently evaluated the imaging datasets according to the proposed imaging quality classification system for CBCTHA and CTHA. Disagreements in interpretation were resolved by consensus.

Statistical Analysis

As the 181 procedures analyzed were performed on 144 consecutive patients, generalized linear modeling including a random subject effect was used to capture the intrapatient correlation. All analyses were performed on the basis of the generalized estimating equations approach of Liang and Zeger [17]. To capture the intrapatient correlation for continuous variables, the unbiased variance–covariance sandwich estimator suggested by Huber and White was

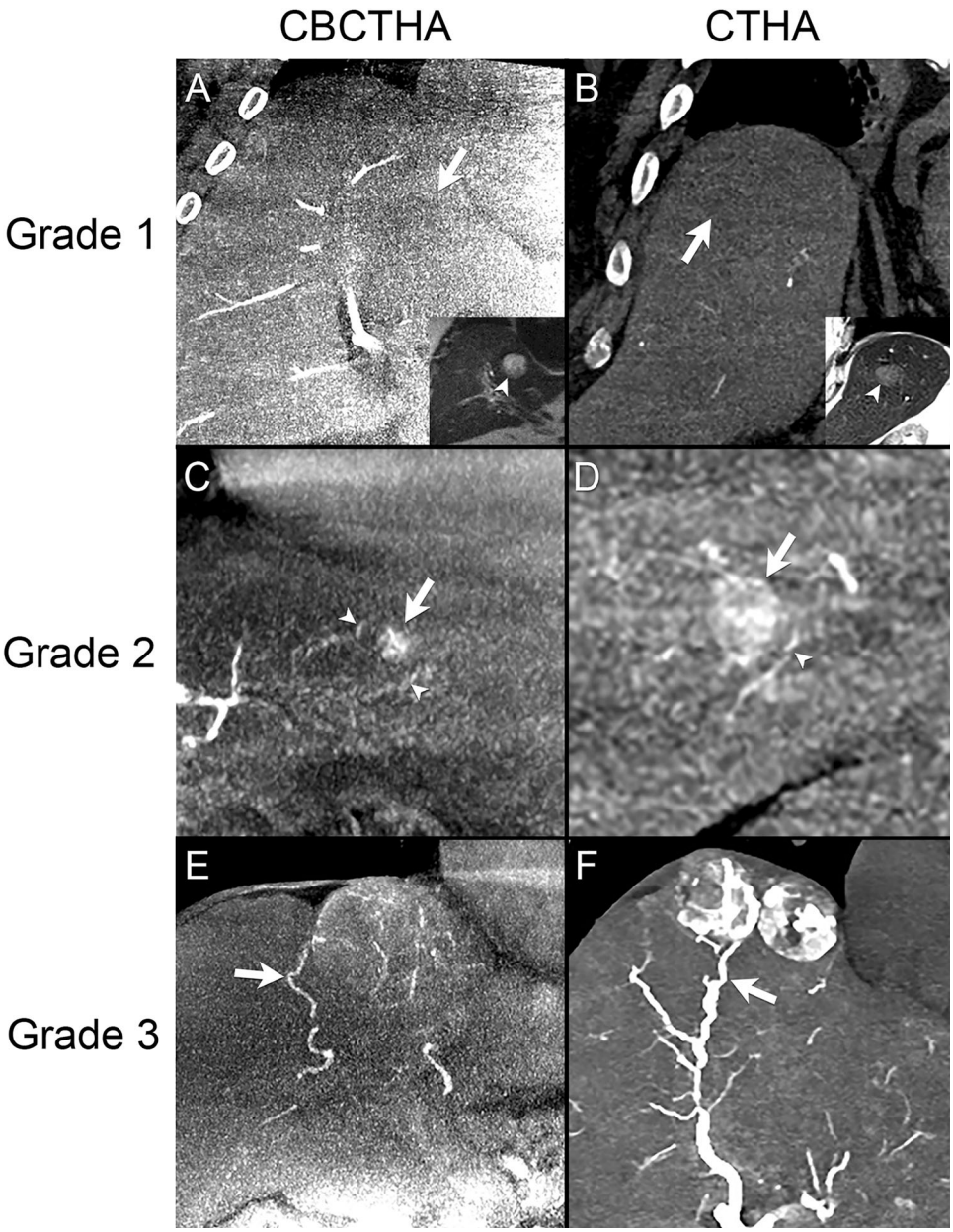

Fig. 3 Representative examples of grades 1–3 tumor feeder vessel identification utilizing 5-mm-thick maximum intensity projection images at a window width of 400 HU and level of 150 HU on coronal CBCTHA and coronal CTHA. **A** A neuroendocrine liver metastasis was poorly visualized on CBCTHA (arrow) but showed high intensity on coronal T2-weighted MRI (inset, arrowhead). **B** A hepatocellular carcinoma (HCC) was poorly visualized on CTHA (arrow) but clearly delineated on coronal T2-weighted MRI (inset, arrowhead). **C**, **D** The feeder arteries (arrowheads) were within 1 cm of the tumors (arrows) without direct contact with the tumors on CBCTHA (**C**) and CTHA (**D**). **E**, **F** The feeder arteries (arrows) directly contacted the tumors on CBCTHA (**E**) and CTHA (**F**)

used [18, 19], and comparisons between CBCTHA and CTHA were made using the generalized estimating equation-based F test. Descriptive statistics for continuous variables are presented as mean ± SD. Categorical variables, including imaging characteristics, are presented as counts and percentages and were compared between CBCTHA and CTHA using the z-score test generated from the generalized estimating equations. $P < .05$ was considered significant. All statistical analyses were performed using SAS 9.4 (SAS Institute Inc.) by a professional statistician with 30 years of experience (J.E.).

Results

Tumor Identification and Tumor Feeder Vessel Identification

Results of qualitative analysis of the identification of tumor and tumor feeder vessel for CBCTHA and CTHA are summarized in Table 3. Excellent (grade 3) tumor identification was recorded in 62 of 111 (55.9%) TACE procedures performed with CBCTHA planning and in 60 of 70 (85.7%) TACE procedures performed with CTHA planning. Moreover, tumors were not detected (grade 1) in 11 of 111 (9.9%) CBCTHA cases, while all tumors were identified (grade 2 or 3) in CTHA cases. Tumor feeder

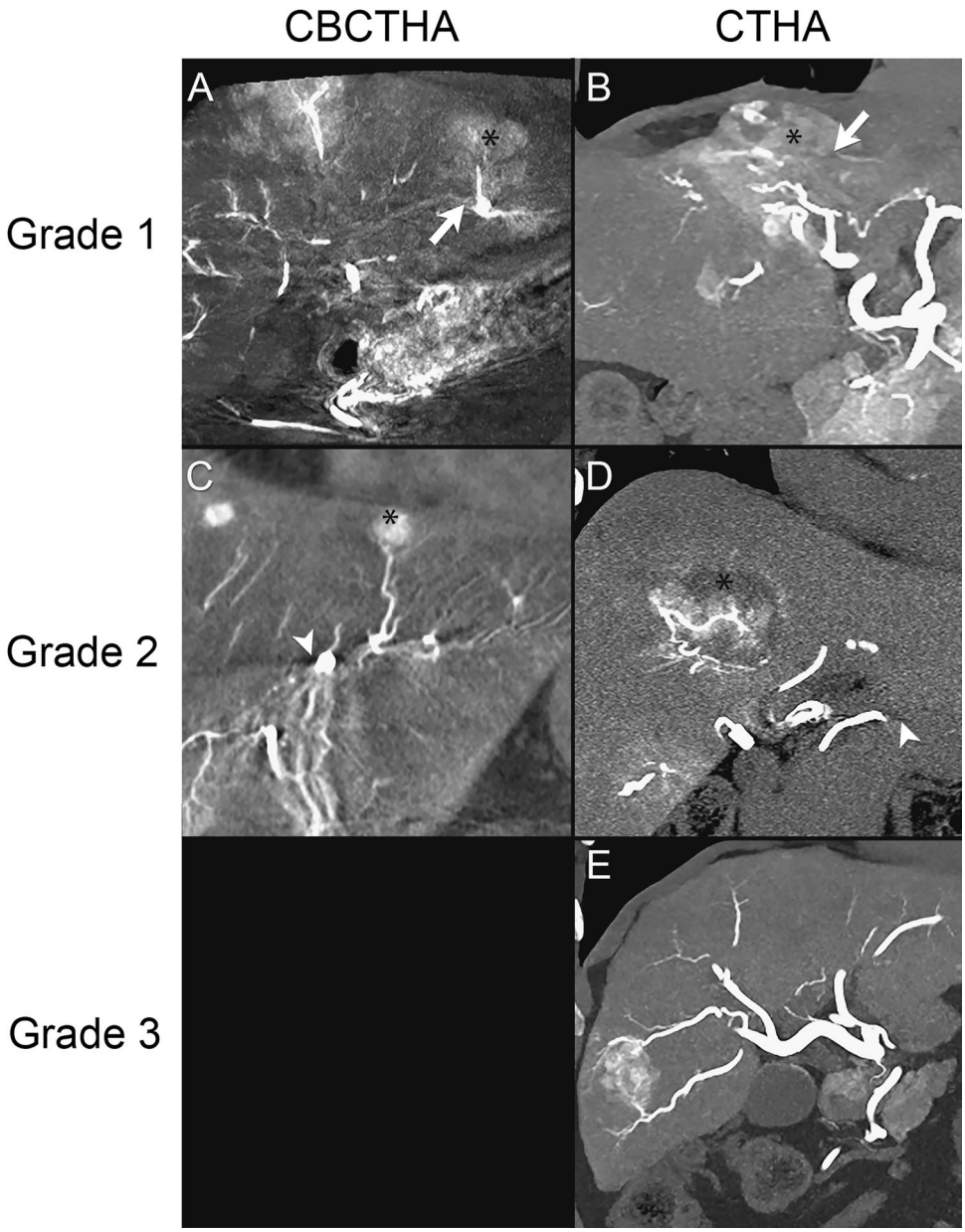

Fig. 4 Representative examples of grades 1–3 streaking artifact on 5-mm-thick maximum intensity projection images at a window width of 400 HU and level of 150 HU on coronal CBCTHA and coronal CTHA. **A**, **B** Presence of streaking artifact (arrows) degraded quality of target tumor (asterisk) images on CBCTHA (**A**) and CTHA (**B**). **C**, **D** Streaking artifact (arrowheads) was present but did not degrade the quality of target tumor (asterisk) images on CBCTHA (**C**) and CTHA (**D**). **E** No streaking artifact on CTHA (No image was free of streaking artifact on CBCTHA.)

vessel identification was optimal (grade 3) in 81 of 111 (73%) CBCTHA cases and in 62 of 70 (88.6%) CTHA cases. Tumor feeder vessels were not visualized (grade 1) in 9% of CBCTHA cases and in 2.9% of CTHA cases.

Presence and Effect of Streaking Artifact, FOV Encompassing the Entire Liver, and Breathing Motion Artifact

Streaking artifact was absent in 55.7% of CTHA cases and 0% of CBCTHA cases ($P < .0001$). The FOV encompassed the entire liver in 84.3% of CTHA cases versus 22.5% of CBCTHA cases ($P < .0001$). A trend ($P = .057$) was noted toward a lower incidence of breathing motion artifact with CTHA, with breathing motion artifact seen in only 1 of 70 (1.4%) CTHA cases versus 11 of 111 (9.9%) CBCTHA cases (Table 4).

Discussion

Adequate tumor visualization and identification of its feeder vessel are two fundamental elements for performing TACE in a safe and effective manner. We demonstrated that CTHA was consistently significantly superior to CBCTHA for TACE planning based on qualitative analysis of tumor identification and tumor feeder vessel identification. Likewise, CTHA also demonstrated significantly

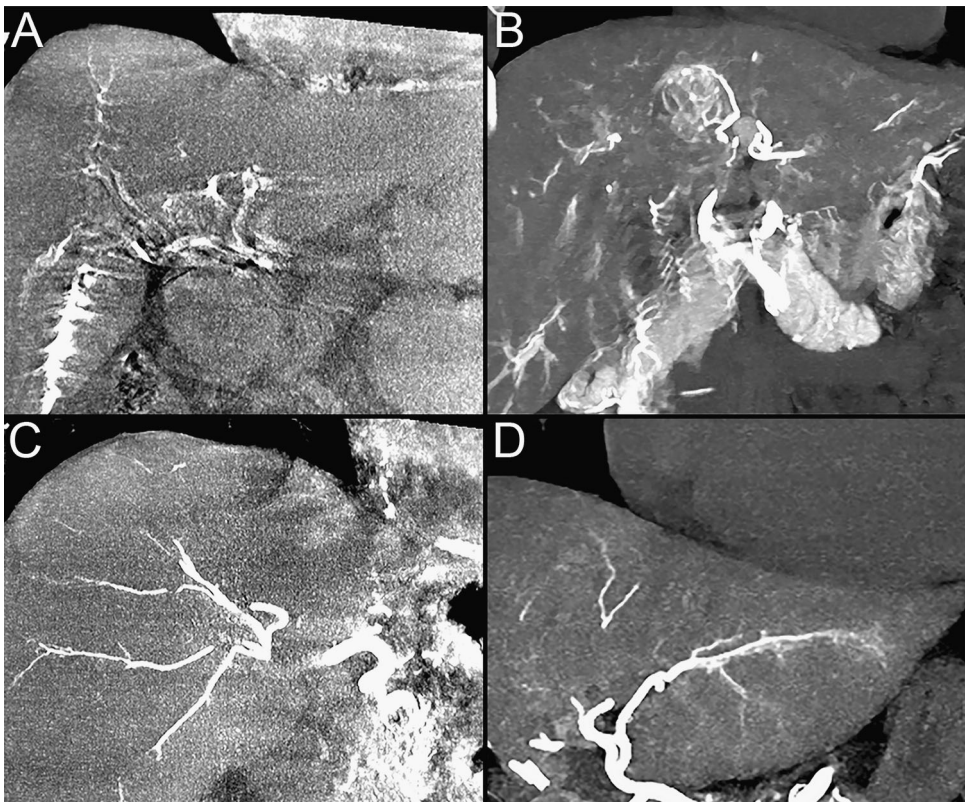

Fig. 5 Representative examples of presence and absence of breathing motion artifact at a window width of 400 HU and level of 150 HU on coronal CBCTHA and coronal CTHA. **A**, **B** Presence of motion artifact results in duplication of vasculatures and organs. The motion artifact on CBCTHA affected the whole image (**A**), while it was limited to the central part of the image on CTHA (**B**). **C**, **D** In the absence of breathing motion artifact, cardiac motion and pulsatile aortic motion remain inevitable on both CBCTHA and CTHA. Nevertheless, images of the lateral segment on CTHA (**D**) are less affected by cardiac motion artifact than are images of the lateral segment on CBCTHA (**C**)

Table 3 Qualitative analysis of imaging quality in CBCTHA (n = 111) and CTHA (n = 70)

Image quality	Qualitative grade			*P* value
	1	2	3	
Tumor identification				< .0001
CBCTHA	11 (9.9)	38 (34.2)	62 (55.9)	
CTHA	0 (0)	10 (14.3)	60 (85.7)	
Tumor feeder vessel identification				< .05
CBCTHA	10 (9.0)	20 (18.0)	81 (73.0)	
CTHA	2 (2.9)	6 (8.6)	62 (88.6)	
Streaking artifact				< .0001
CBCTHA	21 (18.9)	90 (81.1)	0 (0)	
CTHA	1 (1.4)	30 (42.9)	39 (55.7)	

CBCTHA cone-beam computed tomography during hepatic arteriography, *CTHA* computed tomography during hepatic arteriography

Table 4 Categorical analysis of image quality in CBCTHA (n = 111) and CTHA (n = 70)

Variable	No	Yes	*P* value
FOV encompasses entire liver			< .0001
CBCTHA	86 (77.5)	25 (22.5)	
CTHA	11 (15.7)	59 (84.3)	
Presence of breathing motion artifact			.057
CBCTHA	100 (90.1)	11 (9.9)	
CTHA	69 (98.6)	1 (1.4)	

CBCTHA cone-beam computed tomography during hepatic arteriography, *CTHA* computed tomography during hepatic arteriography, *FOV* field of view

improved imaging profile in respect of presence of streaking artifact, and whole liver coverage. Finally, there was also a trend for less breathing motion artifact with CTHA than with CBCTHA.

The advantages of CBCTHA over digital subtraction angiography in patients with HCC for tumor delineation and detection of tumor-feeding arteries for TACE planning are well established [20–24]. A meta-analysis showed that the pooled sensitivity values for tumor and tumor feeder vessel identification were 90% and 91%, respectively, for CBCTHA, versus only 67% and 55%, respectively, for digital subtraction angiography [25]. Despite that our present study also included non-HCC tumors, the pooled sensitivity values of CBCTHA for detecting tumor and tumor feeder vessels were almost identical to the values in the meta-analysis, 90.1% and 91%, respectively. In the early Asian experience, the sensitivity of CTHA was 87% for identification of HCC and 87% for identification of liver metastases [26, 27]. In our study, the pooled sensitivity values for CTHA for tumor identification and tumor feeder vessel identification were 100% ($P < .0001$) and 97.1% ($P < .05$), respectively, better than the values in our internal CBCTHA comparison cohort and the existing literature.

Regarding breathing motion artifact, patient characteristics that could affect breath holding, such as age, body mass index, tumor burden, and prior TACE procedures, were not significantly different between the CBCTHA and CTHA cohorts. Further, our extensive experience with CBCTHA allowed us to minimize motion artifacts in CBCTHA. Therefore, it is likely that the observed trend of higher incidence of breathing motion artifact in CBCTHA than in CTHA is explained by the inherent acquisition differences between these imaging modalities, namely the longer rotation time in CBCTHA and the wide-area X-ray beam used in CBCTHA. Any motion during the CBCTHA gantry rotation time contaminates all projection data instead of only a limited area as in CTHA.

Regarding streaking artifact, only 1.4% of CTHA images versus 18.9% of CBCTHA images had streak artifact affecting image interpretation (grade 1). Undiluted contrast medium caused the majority of streaking. The same undiluted contrast medium was used for both CTHA and CBCTHA. The higher rate of grade 1 streaking artifact in CBCTHA was likely a consequence of the reduced angular (view) sampling in CBCTHA. In our study, CBCTHA images were acquired with patients' arms positioned above the head to decrease the risk of collision and reduce beam hardening artifacts. Because the rotating components are sealed within the gantry in CTHA, CTHA images were acquired with patients' arms alongside the body for increased patient comfort and improved procedure workflow. Despite the potential increase in artifacts from arm positioning in CTHA, streaking artifact degrading image quality (grade 1) was found in only 1 of 70 (1.4%) CTHA cases, versus 21 of 111 (18.9%) CBCTHA cases.

CBCT has lower contrast resolution than traditional CT, primarily because of the large amount of scatter radiation produced by the wide X-ray cone beam [28]. Lower contrast resolution is a disadvantage during TACE as it limits the detection of small tumors with only subtle differences in attenuation between the tumor and nontumoral liver parenchyma. Another advantage of CTHA over CBCTHA is that the large FOV of CTHA enables imaging of the entire liver. Although recent advances in CBCT technology facilitate whole liver imaging, the coverage in Z-axis is still limited and cannot be as flexible as in CT acquisition.

This study has some limitations. First, we did not analyze the impact of CBCTHA and CTHA on local tumor control because of heterogeneous tumor types. Second, radiation dose was not measured since dose metrics reported by CBCT and traditional CT are not directly comparable. However, a lower measured radiation dose in multidetector CT than in CBCT for interventional procedures was suggested in two studies [29, 30] and should be further investigated. Third, contrast injection protocols and imaging acquisition varied among the two cohorts, which might affect imaging characteristics. Finally, because of the smaller FOV on CBCTHA, the higher frequency of catheter positioning distal to the gastroduodenal artery in the CBCTHA cohort might partially explain the higher frequency of streaking artifact due to distribution of denser and more heterogeneous contrast medium.

Conclusion

In conclusion, CTHA is superior to CBCTHA for TACE planning as demonstrated by improved tumor and feeder vessel identification, decreased frequency of streaking artifact, increased frequency of FOV encompassing the whole liver, and a trend for less motion artifact.

Acknowledgements The authors thank Stephanie Deming, an employee of the Department of Scientific Publications, MD Anderson Cancer Center, for copyediting the manuscript. This research was supported in part by the National Institute of Health through MD Anderson's Cancer Center Support Grant, CA016672.

Funding This study was funded in part by the National Institute of Health through MD Anderson's Cancer Center Support Grant, CA016672.

Compliance with Ethical Standards

Conflict of interest Gouthami Chintalapani is an employee of Siemens Healthineers. Bruno C. Odisio has a research Grant from Siemens Healthineers.

Ethical Approval This single-institution retrospective study was compliant with the Health Insurance Portability and Accountability Act and approved by our Institutional Review Board.

Informed Consent For this type of retrospective study, informed consent was waived by our Institutional Review Board.

Consent for Publication Consent for publication was obtained for every individual person's data included in the study.

References

1. Takayasu K, Muramatsu Y, Maeda T, et al. Targeted transarterial oily chemoembolization for small foci of hepatocellular carcinoma using a unified helical CT and angiography system: analysis of factors affecting local recurrence and survival rates. Am J Roentgenol. 2001;176:681–8.
2. Tacher V, Radaelli A, Lin M, Geschwind JF. How I do it: cone-beam CT during transarterial chemoembolization for liver cancer. Radiology. 2015;274:320–34.
3. Wallace MJ, Kuo MD, Glaiberman C, et al. Three-dimensional C-arm cone-beam CT: applications in the interventional suite. J Vasc Interv Radiol. 2009;20:S523–37.
4. Lee IJ, Chung JW, Yin YH, et al. Cone-beam computed tomography (CBCT) hepatic arteriography in chemoembolization for hepatocellular carcinoma: performance depicting tumors and tumor feeders. Cardiovasc Intervent Radiol. 2015;38:1218–30.
5. Inoue A. Development of a hybrid CT/angiography system. Med Rev. 1993;43:9–15.
6. Jaffray DA, Siewerdsen JH. Cone-beam computed tomography with a flat-panel imager: initial performance characterization. Med Phys. 2000;27:1311–23.
7. Ning R, Chen B, Yu R, Conover D, Tang X, Ning Y. Flat panel detector-based cone-beam volume CT angiography imaging: system evaluation. IEEE Trans Med Imaging. 2000;19:949–63.
8. Wallace MJ, Murthy R, Kamat PP, et al. Impact of C-arm CT on hepatic arterial interventions for hepatic malignancies. J Vasc Interv Radiol. 2007;18:1500–7.
9. Araki K, Maki K, Seki K, et al. Characteristics of a newly developed dentomaxillofacial X-ray cone beam CT scanner (CB MercuRay): system configuration and physical properties. Dentomaxillofacial Radiol. 2004;33:51–9.
10. Finkenstaedt T, Morsbach F, Calcagni M, et al. Metallic artifacts from internal scaphoid fracture fixation screws: comparison between C-arm flat-panel, cone-beam, and multidetector computed tomography. Invest Radiol. 2014;49:532–9.
11. Toyoda H, Kumada T, Sone Y. Impact of a unified CT angiography system on outcome of patients with hepatocellular carcinoma. AJR Am J Roentgenol. 2009;192:766–74.
12. Iwazawa J, Ohue S, Hashimoto N, Muramoto O, Mitani T. Survival after C-arm CT-assisted chemoembolization of unresectable hepatocellular carcinoma. Eur J Radiol. 2012;81:3985–92.
13. Takada K, Toyoda H, Tada T, et al. Accurate and rapid identification of feeding arteries with multidetector-row angiography-assisted computed tomography for transarterial chemoembolization for hepatocellular carcinoma. J Gastroenterol. 2015;50:1190–6.
14. Tanaka T, Arai Y, Inaba Y, et al. Current role of hybrid CT/angiography system compared with C-arm cone beam CT for interventional oncology. Br J Radiol. 2014;87:20140126.
15. Schegerer AA, Lechel U, Ritter M, Weisser G, Fink C, Brix G. Dose and image quality of cone-beam computed tomography as compared with conventional multislice computed tomography in abdominal imaging. Invest Radiol. 2014;49:675–84.
16. Kohlbrenner R, Kolli KP, Taylor AG, et al. Patient radiation dose reduction during transarterial chemoembolization using a novel X-ray imaging platform. J Vasc Interv Radiol. 2015;26:1331–8.
17. Liang KY, Zeger SL. Longitudinal data-analysis using generalized linear-models. Biometrika. 1986;73:13–22.
18. Huber PJ. The behavior of maximum likelihood estimates under nonstandard conditions. In: Proceedings of the fifth Berkeley symposium on mathematical statistics and probability, volume 1: statistics. Berkeley, California: University of California Press; 1967. p. 221–33.
19. White H. A heteroskedasticity-consistent covariance-matrix estimator and a direct test for heteroskedasticity. Econometrica. 1980;48:817–38.
20. Kakeda S, Korogi Y, Ohnari N, et al. Usefulness of cone-beam volume CT with flat panel detectors in conjunction with catheter angiography for transcatheter arterial embolization. J Vasc Interv Radiol. 2007;18:1508–16.
21. Minami Y, Yagyu Y, Murakami T, Kudo M. Tracking navigation imaging of transcatheter arterial chemoembolization for hepatocellular carcinoma using three-dimensional cone-beam CT angiography. Liver Cancer. 2014;3:53–61.
22. Iwazawa J, Ohue S, Mitani T, et al. Identifying feeding arteries during TACE of hepatic tumors: comparison of C-arm CT and digital subtraction angiography. AJR Am J Roentgenol. 2009;192:1057–63.
23. Miyayama S, Yamashiro M, Hashimoto M, et al. Identification of small hepatocellular carcinoma and tumor-feeding branches with cone-beam CT guidance technology during transcatheter arterial chemoembolization. J Vasc Interv Radiol. 2013;24:501–8.
24. Iwazawa J, Ohue S, Kitayama T, Sassa S, Mitani T. C-arm CT for assessing initial failure of iodized oil accumulation in chemoembolization of hepatocellular carcinoma. AJR Am J Roentgenol. 2011;197:W337–42.
25. Pung L, Ahmad M, Mueller K, et al. The role of cone-beam CT in transcatheter arterial chemoembolization for hepatocellular carcinoma: a systematic review and meta-analysis. J Vasc Interv Radiol. 2017;28:334–41.
26. Murakami T, Oi H, Hori M, et al. Helical CT during arterial portography and hepatic arteriography for detecting hypervascular hepatocellular carcinoma. AJR Am J Roentgenol. 1997;169:131–5.
27. Inaba Y, Arai Y, Kanematsu M, et al. Revealing hepatic metastases from colorectal cancer: value of combined helical CT during arterial portography and CT hepatic arteriography with a unified CT and angiography system. AJR Am J Roentgenol. 2000;174:955–61.
28. Al-Ekrish AA, Ekram M. A comparative study of the accuracy and reliability of multidetector computed tomography and cone beam computed tomography in the assessment of dental implant site dimensions. Dentomaxillofacial Radiol. 2011;40:67–75.
29. Jones AK. An apples to apples comparison of radiation dose and image quality between flat panel CT and multidetector CT. In: Presented at society of interventional radiology 2018 annual scientific meeting, Los Angeles; 2018.
30. Steuwe A, Geisbusch P, Schulz CJ, Bockler D, Kauczor HU, Stiller W. Comparison of radiation exposure associated with intraoperative cone-beam computed tomography and follow-up multidetector computed tomography angiography for evaluating endovascular aneurysm repairs. J Endovasc Therapy. 2016;23:583–92.